Haptic Interfacing in Animal Behavioral Systems: Implications for Motor Rehabilitation

BY

ASHLEY V. GREENE
B.S.E. Arizona State University, Tempe, AZ, 2007

THESIS

Submitted as partial fulfillment of the requirements
for the degree of Master of Science in Bioengineering
in the Graduate College of the
University of Illinois at Chicago, 2012

Chicago, Illinois

Defense Committee:

James Patton, Chair and Advisor
David Vaillancourt, Kinesiology and Nutrition
Richard Magin

Table of Contents

TABLE OF FIGURES

TABLE OF FIGURES (continued)

SUMMARY

Parameters such as speed, position, movement direction, and force have been reported to independently and dependently alter neural activity in the motor cortex (M1). Many types of animal behavioral tasks have been designed to associate these desired kinematic or spatiotemporal parameters with M1 neural activity. However, to date, minimizing undesired movement variation of animals performing behavioral tasks has not been achieved. Moreover, behavioral systems to date have not been utilized on overtrained animals in order to study the effects of a learned behavior on M1 activity prior to, and following, motor cortical injury.

Haptics interfacing, a platform commonly used in human motor retraining, affords adaptability to independent changes in targeted kinematic or dynamic parameters with relative ease; thereby encouraging movement repeatability. This platform was used in a novel animal behavioral-brain-machine interface (BMI) to inhibit undesired movement variation. Utilization of a haptics system as an animal behavioral-BMI in a preliminary pre-to post-stroke study has shown task performance repeatability, in addition to revealing that the threshold for neural activity baseline deviation increases in response to change in neural behavioral-influencing parameters as a result of performing a learned behavior. Additionally, neuronal excitability in the M1 following focal cortical infarction showed dependence on location relative to the site of infarction.

Further studies are needed in overtrained animals prior to M1 injury to observe the neural response to a learned behavior, in order to gain a better understanding of M1 activity stability. Furthermore, future studies in overtrained animals following M1 injury are needed, and should focus on observing changes in neuronal excitability, relative to location from infarct site, in order to improve localized treatment methods for motor rehabilitation.

INTRODUCTION

In recent years, haptic interfacing has gained popularity as a rehabilitation tool for human motor function recovery. Haptic interfacing is defined as a platform that uses tactile and force-rendering to enable the user to receive tactile feedback from interaction with a virtual environment. Haptic systems provide sensory feedback, can be coupled with other software to obtain kinematic feedback, can introduce force fields and monitor position, and can be customized to target retraining for a wide variety of upper extremity motor impairments (Holden, 2005). Virtual environments and tasks can be modified fairly easily according to changing patient needs, but the options for just how to perform the best treatment and training are vast and risk never being fully determined. Animal models offer an excellent way to hasten the scientific process in rehabilitation, providing opportunities for rapid evaluation, monitoring of concurrent brain activity, and understanding the underlying physiology of recovery at all levels.

Moreover, motor retraining has been shown to influence motor cortical reorganization in neurological disease affecting motor function. In 1966, Evarts first reported that neural discharge in the motor cortex of a monkey was altered just prior to a movement. Activity of neural cells in the primary motor cortex (M1) was later found to be dependent on specific movement variables. M1 neural cells of animal models have exhibited preferential behavior in relation to varied attributes of movement, such as direction of motion, speed (Ashe & Georgopoulos, 1994; Moran & Schwartz, 1999), or force (Ashe, 1997; Georgopoulos *et al*., 1992). For this reason, attributes of haptic systems, such as acquiring and maintaining some established control over, or monitoring, movement kinematics such as direction of motion, position and speed, is also essential in animal behavioral systems for observing the neurophysiology of the motor cortex.

A variety of animal behavioral tasks have been implemented with the aim of observing the effects of specific kinematic or spatiotemporal parameters on neural behavior in the M1. The center-out

task method (Georgopoulos *et al*. 1982; Moran & Schwartz 1999) requires the animal to successfully reach eight pseudorandom, equally-spaced radial targets. However, the only instituted task control (task control is defined as predetermined modifications of a behavioral task that are incorporated to inhibit undesired variability in an animal's movements) of this method is incorporating time constraints. Modifications of the center-out task method to incorporate force ramping in the plane of targeted motion (Sergio *et al.* 2005) introduced greater control over speed variability, but control over spatial variability remains minimal. Paninski and colleagues (2004) designed the pursuit-tracking task (PTT) to control the animal's movements by requiring constant pursuit of a cursor, but the PTT was unable to reduce uncertainty in the temporal relationship between movement variables and M1 neural cell firing. Moreover, rat behavioral tasks aimed to observe the relationship between movement and M1 behavior or M1 reorganization as a result of cortical injury or motor skill acquisition have been limited to uncontrolled skilled reaching and lever-press tasks (Kleim *et al.* 1998; Chapin *et al.* 1999; Whishaw & Pellis 1990; Ballermann *et al.* 2000; Metz & Whishaw 2000; Laubach *et al.* 2000; Jensen & Rousche 2006). Responding to this need, our goals were to develop a three-dimensional interface for recording behavior and cortical activity with minimal spatial and speed variability that also allows the operator to alter the virtual environment.

Additionally, a clear need in rehabilitation is to expand such capabilities to also study the recovery process following brain injury. Motor skill acquisition and motor retraining due to disease or injury are widely known to induce considerable neuroplasticity in the corresponding M1 representation areas, and motor retraining for recovery of activities of daily living is ideal for understanding relevant motor patterns. In a study of the stability of M1 functional maps in early and posttrained monkeys, Plautz and colleagues (2000) imply that, as a result of overtraining, functional M1 maps may return to baseline conditions once the skill becomes a learned behavior. To the best of our knowledge, animal behavioral studies utilizing neuronal recordings that do not incorporate complex tasks such as sequential

movement memorization (Lu & Ashe, 2005; Matsuzaka, Picard & Strick, 2007), have not studied the effect of injury on the neural-behavioral relationships in overtrained animals.

As a result of motor skill training, M1 firing has been reported to show increased reliability and decreased firing rates pre- and post-task related bursts of activity over time (Kargo & Nitz, 2004). The study of Kargo & Nitz only extended through 12 days of behavioral training, and M1 firing reliability improvements continued on the final training day. No reports have been found that address whether M1 firing activity, in response to long-term behavioral training, reaches a level of stabilization.

The study presented in this thesis aimed to use a haptic interface system, through use of a haptically rendered virtual environment, to address the question of whether subpopulation level (subpopulation is defined as all neurons found on a single electrode) M1 activity of overtrained animals exhibits day-to-day stability, implying that a baseline for M1 activity may exist for motor skills and patterns of learned behaviors. The system designed and utilized in this study minimized undesired spatial and speed variability by using a one-dimensional behavioral task. Preliminary results obtained demonstrated subpopulation M1 activity responding only to sudden changes in M1-affecting parameters in response to a learned behavior; in addition to the effects of subsequent M1 infarction. These results introduce a system for developing animal behavioral tasks that further encourages movement repeatability, thus minimizing M1 firing variability resulting from trajectory deviations or inconsistent trial speeds. Moreover, they confirm differences between the M1 behavioral response to learned behaviors and short-term practiced tasks.

Preliminary pre-and post-stroke results have been obtained on the utilization of photothrombotic stroke induction in the forelimb M1 representation area, in order to observe the neuroplastic changes to M1 activity during retraining of a previously learned behavior. These results have shown a change in neuronal excitability that is dependent on the distance from the induced focal infarct area.

METHODS

Preliminary experiments were performed using male Sprague-Dawley rats (450-500 g; Harlan, Inc.) with the haptic system (non-implanted; n=10), and full system (implanted; n=4), trained to complete the behavioral task outlined in a following section. Rats were held between 80-85% of free-feeding body weight, and were allowed free access to water. Electrode implantation surgery was performed after animals had been fully trained for 10-11 months. Behavioral task motivation was limited to 45 mg purified diet pellets (Bio-Serv, Inc.).

Electrode design and manufacture

Microwire electrode arrays, with 3 x 2 rectangular configuration, of Teflon-coated 100 μm tungsten wire (A-M Systems, Inc.), with sealed stroke tube, were developed using a custom-designed jig (manufactured by RJM Rapid Prototyping; interelectrode distance: 650 μm; center-to-center distance between stroke tube and Column 1 electrodes: 960 μm) (Fig. 1A). The stroke tube was defined as a 720 μm outer diameter polyimide tube used as a portal for cortical infarction induction via photothrombosis in a chronically recorded animal. Prior to electrode assembly, a layer of parafilm was placed on the jig to facilitate separation of the electrode from the jig during electrode fabrication. Prior to placing the tungsten wire for each electrode, a 279 μm diameter polyimide tube (length = 1 cm) was inserted midway through an electrode hole in the jig and followed by a smaller polyimide tube (diameter = 160 μm; length = 1.5 cm) to ensure mechanical stability. After the tubing for the six electrodes has been positioned, the stroke tube (length = 2 cm) was placed midway through the jig, and a single layer of parafilm was used to protect the brain from the environment by placing it over the stroke tube's opening on the brain side. A thin layer of dental acrylic was then laid and allowed to cure around the polyimide tubing for the stroke tube and array to facilitate separation of the electrode from the jig. Once the tubing has set in place and been separated from the jig, a tungsten wire (length = 4 cm) was inserted into the 160 μm diameter polyimide tube for each of the six electrode placements leaving 1.8 mm length, relative

to the stroke tube, for implantation. Epoxy and dental acrylic was then placed and allowed to cure around each microwire electrode to prevent wire movement.

After allowing the epoxy and dental acrylic to cure, each microwire was soldered to a single pin in an 8-pin connector, followed by soldering of a 179 µm diameter Teflon-coated tungsten grounding wire (length = 5 cm) with an affixed stainless steel flat washer (outside diameter = 3.8 mm) (McMaster-Carr Supply Co.) to the seventh and eighth pin. When connected to the neural recording system, pins seven and eight were automatically grounded. The grounding wire was included to minimize in-session noise due to loose or disconnected grounding.

Two layers of parafilm are then placed over the end of the stroke tube exposed to the environment. Dental acrylic and epoxy are used to insulate the microwire electrodes and protect the microwire-connector connection from damage. A 2 cm length of the grounding wire, with affixed washer, remained free from dental acrylic and epoxy for placement around a bone screw during implantation surgery. 3 mm of the stroke tube was left partially exposed to the environment, with the opening covered by a double layer of parafilm and a thin layer of dental acrylic to further protect the brain from the environment and allow access of the fiber-optic light probe during stroke induction (Fig. 1B).

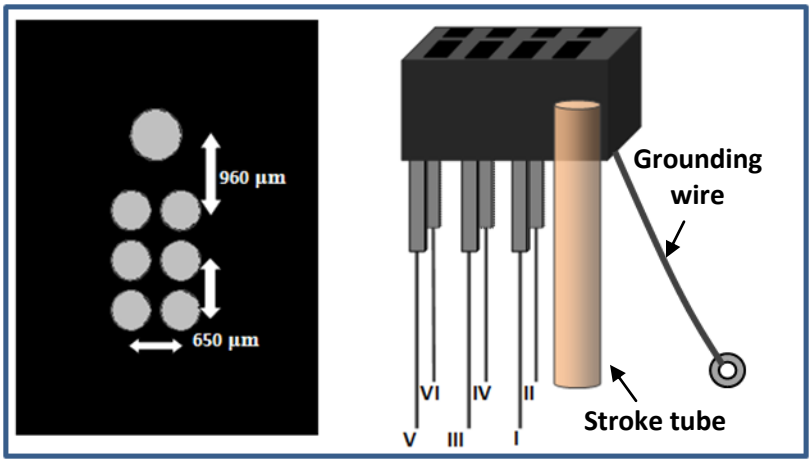

Figure 1: Left: Jig used to place microwire electrode array and stroke tube. Right: Schematic representation of the 3x2 microwire electrode array with stroke tube used for each implantation. Numbers indicate electrode placement.

Behavioral task

The behavioral task environment was developed using H3D (SenseGraphics, Inc.) haptics platform with Python programming language (Python Software Foundation). Five virtual walls with haptic rendering were designed to create and enclose the task environment to a one-dimensional space (height = 3 cm; width = 11 cm; depth = 3 cm) as illustrated in Figure 2A. Dynamic constraints were instituted to prevent z directional movement variation and to encourage movement repeatability. Sampling rates from previous animal studies found to have kinematic sampling rates averaging 50-100 Hz. At rest, the kinematic sampling rate observed in this study was 130 Hz, and up to 469 Hz during robot movement.

Rats were fully trained once they were able to reach 2 cm out of a 2.1 x 6 cm opening in the training cage (enclosed in a Faraday cage) to grasp and advance a modified Falcon robotic arm (Novint, Inc.) toward a virtual target (Fig. 2A, D). The virtual target was a 2 cm diameter sphere centered 7 cm horizontally from Barrier 1. The food reward was immediately dispensed once the robot-controlled virtual cursor reached the first target boundary (TB1), which is defined as the target boundary threshold. Animals were conditioned, upon hearing the sound of the food reward dispenser, to release the robot handle and allow the system to return the handle to start position, which is illustrated in Figure 2A. Once TB1 was successfully reached, the target was disabled for 2 s, prohibiting food reward for target hits and further trial advancement. In addition to the 10 N of negative z directional force, an opposing horizontal force was incorporated to minimize speed variability. The maximum amount of opposing force instituted on the animal during the task was 2 N. However, the opposing force was programmed to progressively increase throughout each trial. The opposing force is best estimated in the following equation:

$$\boldsymbol{F(x) = 20\frac{N}{m} * |Ax - Bx|}$$

where Ax is the value of x position at the start of the trial and Bx is the value of the x position, in meters, at any sampled time during a trial.

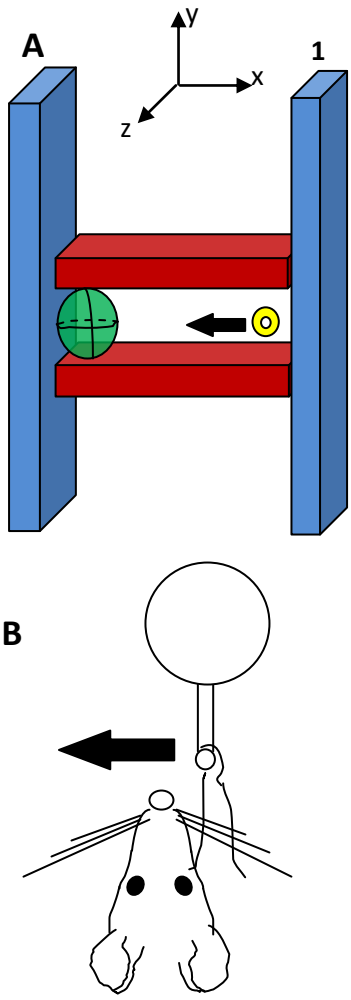

Figure 2: Experimental setup. ***A***: Virtual environment. The yellow circle illustrates the cursor, allowing visualization of animal-controlled handle movement. Barrier 1 indicated with number 1. The rear barrier has been omitted for visual clarity. ***B***: Top view of rat performing the one-dimensional task.

Surgical procedure

Animal experimental procedures were performed in compliance with AAALAC accredited Animal Care Committee of the University of Illinois at Chicago under Protocol #08-013. Animals were anesthetized via a bolus intramuscular injection of ketamine (100 mg/kg), xylazine (5 mg/kg) and acepromazine (2.5 mg/kg) (KXA) in a dose of 0.1 mL/100 g for induction, and thereafter given supplemental intramuscular injections of KXA as needed and indicated by paw-pinch reflex. Oxygen saturation and pulse rate were also continuously monitored throughout the procedure to maintain an appropriate level of anesthesia.

Access to the skull was achieved using a 2 cm midline incision. One stainless steel bone screw was inserted anteriorly into the contralateral hemisphere, and one screw was positioned posteriorly in the ipsilateral hemisphere of the skull before beginning the craniectomy. The craniectomy was performed over the forelimb representation area of the M1, targeted at 1-2.5 mm anterior and 2-3.5 mm lateral to the bregma (Neafsey, 1990). Dura was then withdrawn from the area before placing the microwire array into the micromanipulator for implantation. Immediately prior to implantation, the grounding wire with attached washer was screwed around a third bone screw using a hex nut to secure connection before inserting the bone screw posteriorly into the contralateral hemisphere. After insertion of the final bone screw, the microwire array was implanted at a depth of 1.5 mm beneath the cortical surface. Collagen-based gelfoam was then placed over any exposed brain, and the electrode and bone screws were encapsulated with dental acrylic leaving only the connector visible. Animals were given

seven days recovery to allow bone growth to increase bone screw stability before beginning the full system behavioral task.

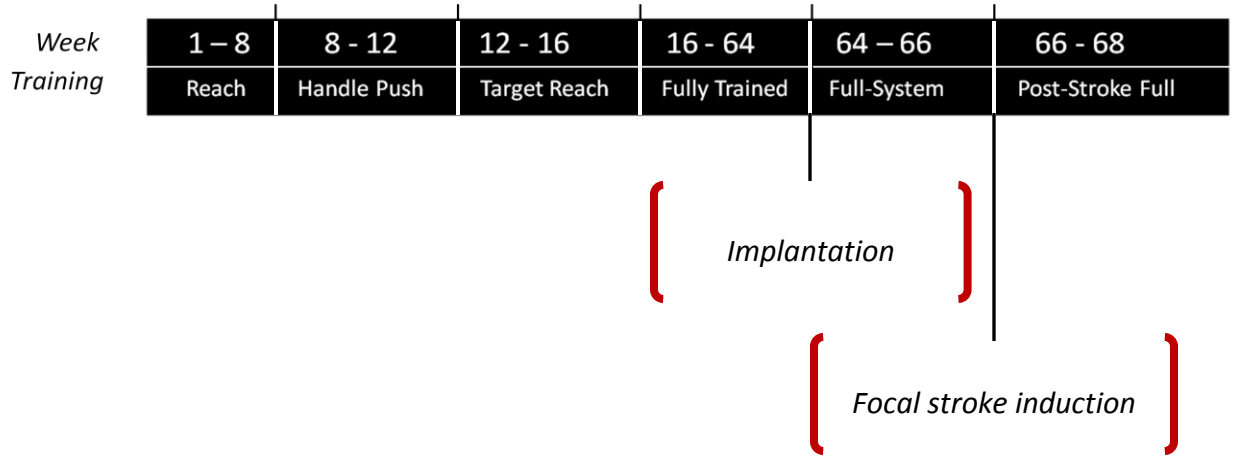

Figure 3: Behavioral training timeline. Approximate time of implantation and focal stroke induction are shown at 64 and 66 weeks, respectively.

Behavioral training

As previously stated, the animals were fully-trained for 10-11 months before implantation. Figure 3 illustrates an approximate timeline for training and system progression.

Electrophysiological recordings and system analysis

Subpopulation neural activity was recorded using a multi-channel recording system (Tucker-Davis Technologies, Inc.; TDT). Neural signals were sampled at 25 kHz and filtered between 300-3000 Hz, and intra-cortical data was saved for off-line analysis. Synchronization with kinematic and dynamic data was completed off-line in MATLAB (The MathWorks, Inc.).

On-line subpopulation spikes were detected using a threshold of 1.5 signal-to-noise (SNR) ratio. Off-line, principal component analysis (PCA) in conjunction with k-means clustering was used on spike waveform samples taken during a period of in-session animal rest to minimize the likelihood of noise using a custom MATLAB routine. Waveforms classified as spikes were then used as reference waveforms for PCA/k-means clustering spike sorting of in-session thresholded neural activity.

ActiveX controls provided by TDT allow client programs, such as programming languages, to access the neural system hardware and stored data. Synchronization of spike timestamps and kinematic data was feasible by introduction of a time shift to the spike timestamps (accuracy of 0.0001 s) to coincide with session start time of the haptic system. Synchronization of spike timestamps with kinematic data, and quantitative analysis of synchronized data, were carried out using custom MATLAB routines. Eight sessions from each overtrained animal pre-stroke, and eight sessions of Rat I post-stroke, averaging 90 trials per session, were assessed in total for the full-system.

Cortical infarction induction

Focal cortical infarction was induced using a photothrombosis procedure modified from Chiganos *et al*. (2006). A winged-tip catheter was inserted into the tail vein 3-6 cm from tail-tip for later injection of rose-bengal (RB) dye. A saline-filled syringe was attached to the catheter to reduce the risk of thrombosis. The layers of dental acrylic and parafilm were then removed from the stroke tube to allow access of the fiber-optic light probe (Intralux 6000, Volpi Inc.). The fiber-optic light probe (outside diameter = 400 μm), tip cleaned with 70% isopropyl alcohol, was lowered into the stroke tube, penetrating the parafilm layer located on the brain side, until the cortical surface was reached. RB dye solution (Aldrich Chemicals; 10 mg/ml, 0.9% saline solution, 2 mg/100 mg body weight) was injected at 1.0 ml/min as the brain surface was illuminated. Illumination proceeded for 20 min following RB injection. The stroke tube was resealed with two layers of parafilm and a layer of dental acrylic once the induction was complete.

RESULTS

Full-system data sets were only obtained from two of the four rats due to complications from surgery, such as weakened bone growth surrounding bone screws. Two of six electrodes from Rat I and four of six electrodes from Rat II were excluded from analysis as a result of subpopulations from each electrode having maximum amplitudes of no more than 50 μV or spike thresholds less than 1.5 SNR for

the duration of session 1. Results presented in this thesis that utilized the method of binning averaging speed or instantaneous firing rate (IFR) over a specified position range did not include bins with data points of less than 10 per position range.

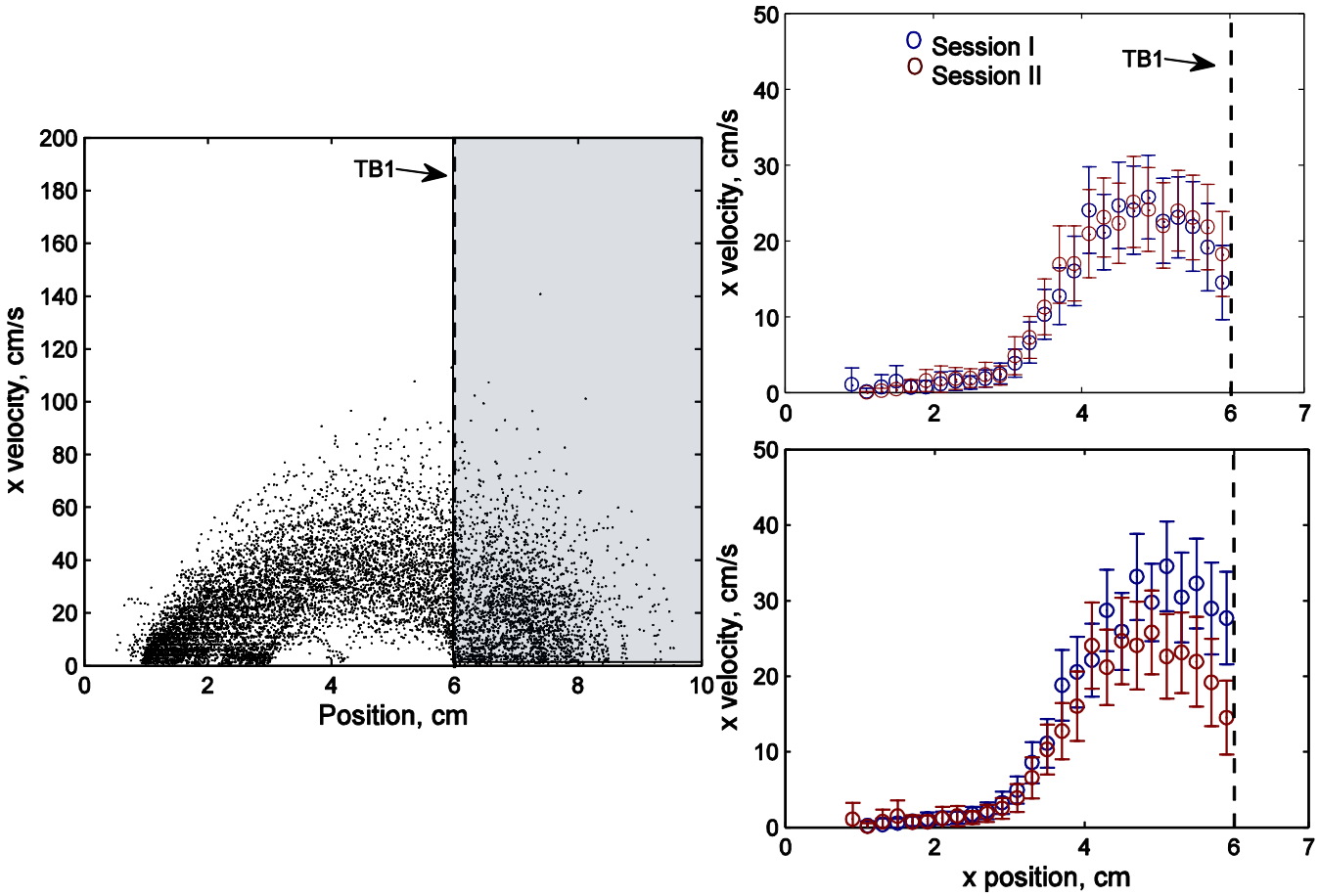

Figure 4: A typical rat's phase plane aspects for handle movements. ***A***: Representative scatter plot of averaged horizontal velocity per 2 mm. ***B***,***C***: Two consecutive day sessions of averaged handle phase plane (velocity vs. position) up to TB1, with 95% confidence interval. (B) Typical repeatability of task performance. (C) Illustrates the worst-case for repeatability from one day to the next. The typical task repeatability, as presented in (B), shows complete overlap of handle speed with respect to position for two consecutive days up to TB1. Overlap is still present in the least repeatable consecutive day performance (C).

Behavioral task

The haptic behavioral system described in this study was designed for use as a one-dimensional task, with a high kinematic sampling rate, that encourages movement repeatability. The deviation from mean of the y and z-directional path was found to be minimal (averaging -0.1028 +/- 0.0009 and -0.0558 +/- 0.0018, respectively). Due to the return x-directional force being dependent on

the final force in the direction of the target, the starting x position commonly varied slightly between 1 cm and 3 cm from zero, with zero being at Barrier 1.

As a result of restricting the task to one-dimension, the velocity was also one-dimensional. Movement repeatability during the behavioral task, defined by overlapped horizontal velocity paths, for consecutive day sessions was typical for all rats using the haptic system (Fig. 4B). In the most session-repeatable cases for each animal, the difference in mean velocity paths, with exclusion of the 95% confidence interval, between Session I and Session II produced P-values of 0.9108 and 0.9252 (Rat I and Rat II, respectively) (paired t-test). The repeatability of task performance is attributed to the opposing force. Non-comparable velocity paths, with differences in mean resulting in a P-value of less than 0.0001 (paired t-test), occurred only once per animal (Fig. 4C).

Pre-stroke subpopulation neural behavior during task

The high kinematic sampling rate of the system allowed synchronization of the kinematic and neural recording data. As shown in Figure 5, the IFR with relation to time does not provide any spatial information about the task. Synchronization of these two data provides more specific information into the relationship between neural behavior and movement. Figure 5B is a typical representation of IFR with respect to time that illustrates the relationship between the session-averaged subpopulation IFR per 10 ms during each trial, proceeding from 500 ms prior to handle movement onset to the end of trial.

While the neural behavior and time relationship well illustrates the subpopulation peri-handle movement onset firing trend, there is no movement information on the task itself, which is essential if there is any intratrial velocity variation. However, the IFR and time relationship does show that, even with consistent change in necessary force output, the averaged subpopulation IFR returns to pre-task baseline level as the task progresses, suggesting that subpopulation level neural activity of an animal performing a learned behavior only changes in response to sudden change in a movement parameter(s), such as speed, direction of motion, or position (Fig. 5B). To complement the information found by observing the neural behavior in relation to peri-handle movement onset time, and to gain spatial

information on neural behavior during the task, the relationship between neural behavior and horizontal handle position was studied. Figure 5A is a representative example of the session-averaged subpopulation IFR per 5 mm using the horizontal position mirrored over zero.

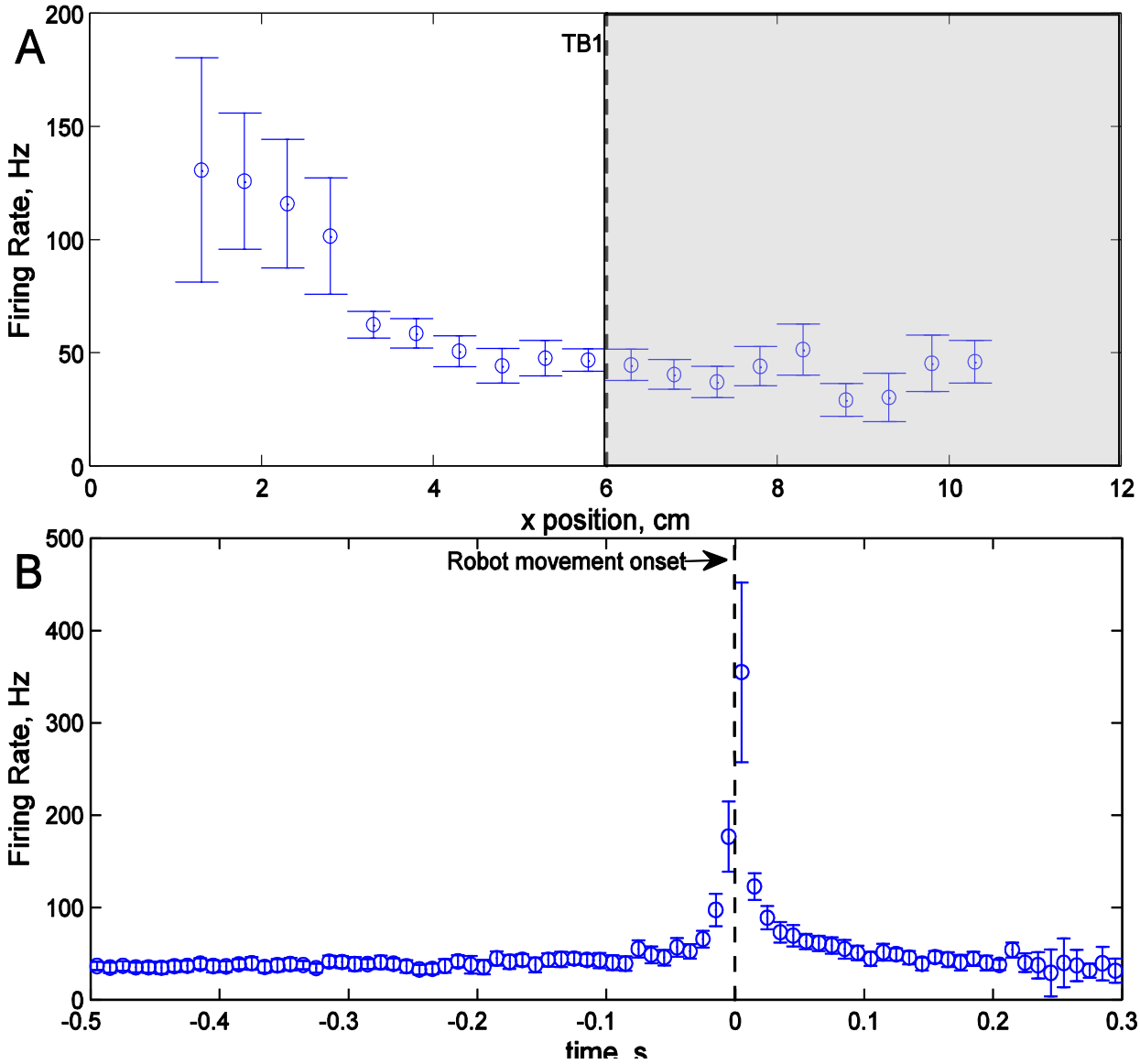

Figure 5: Typical systematic relationships between movement and instantaneous firing rates (IFR). ***A***: Single, typical electrode subpopulation plotted as IFR vs. Position: IFR averaged across 5 mm position ranges, including 95% confidence interval. Gray area encloses the target range. Starting position varies slightly from 0.01 m – 0.03 m. ***B***: Single, typical electrode subpopulation plotted as IFR vs. Time: IFR averaged across 10 ms bins, including 95% confidence interval. Zero is the time of robot movement onset. The mirrored x-position version of the IFR vs. position plot shown for clarity.

Day-to-day and Inter-electrode subpopulation neural behavior during task

The subpopulation-firing trend of increased neural activity as a consequence of sudden change in forelimb position, velocity and direction, but decreasing to a pre-movement baseline level, was

consistent throughout the eight pre-stroke sessions for Rat I and Rat II. As illustrated in Figure 6, with the exception of one session with Rat I, the firing rate trend of increased initial IFR followed by a return to pre-movement baseline remained constant between animals. As shown in Figure 4B, session performance was typically repeatable. Cross-correlations on day-to-day subpopulation neural activity for each electrode, in addition to inter-electrode subpopulation activity, did not reveal any direct correlation in firing between subpopulations, or consistent firing patterns. It is unknown whether synchronized firing would be found if individual neurons were observed as opposed to subpopulations.

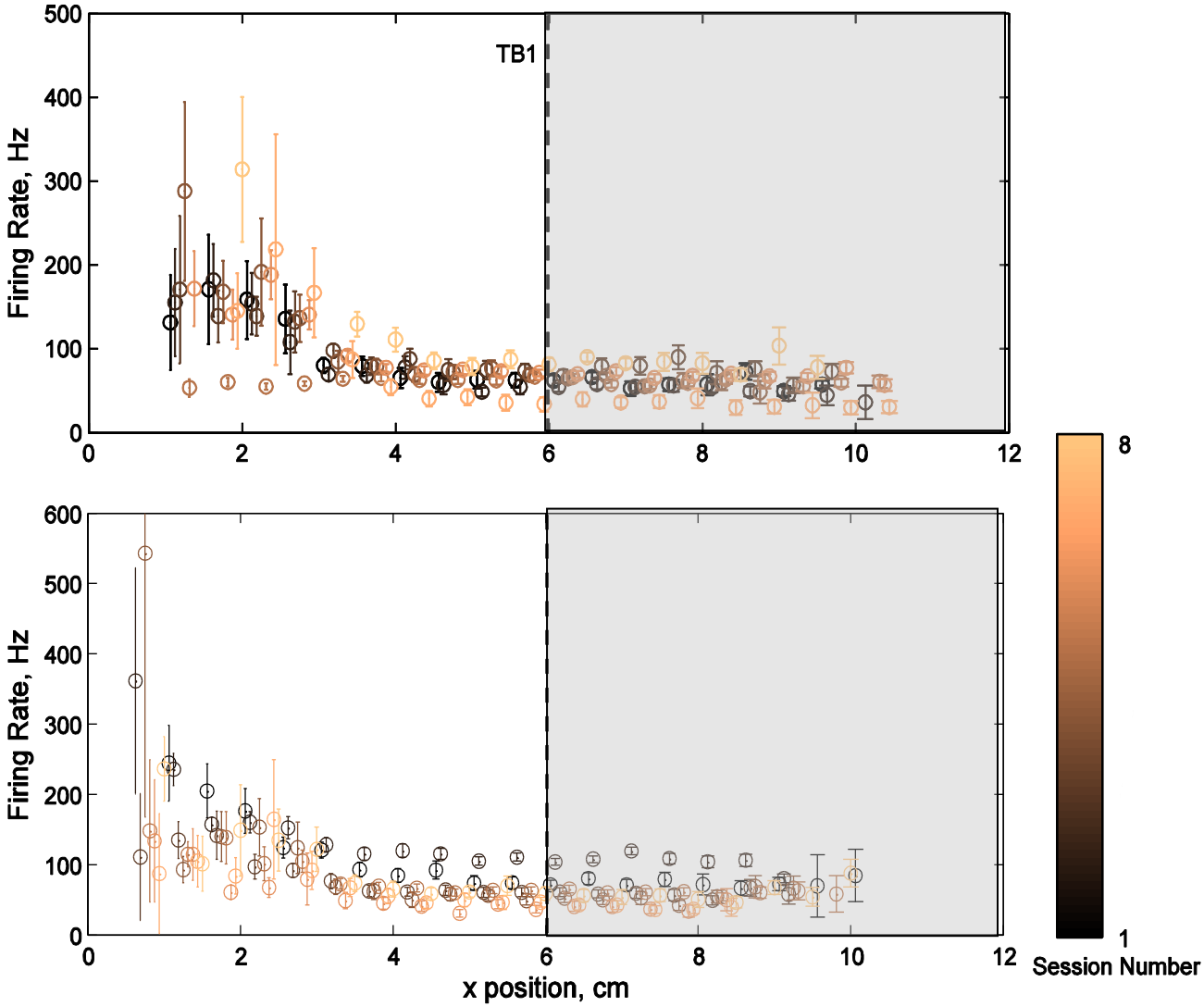

Figure 6: Averaged-session IFR for two rats. Mean IFR per 5 mm. ***A***: Eight pre-stroke sessions of Rat I from Electrode I placement. ***B***: Eight pre-stroke sessions of Rat II from Electrode I placement. Days are slightly staggered in position for better visual clarity. Neural activity from both overtrained rats exhibit the same firing trend that is persistent throughout the eight pre-stroke sessions.

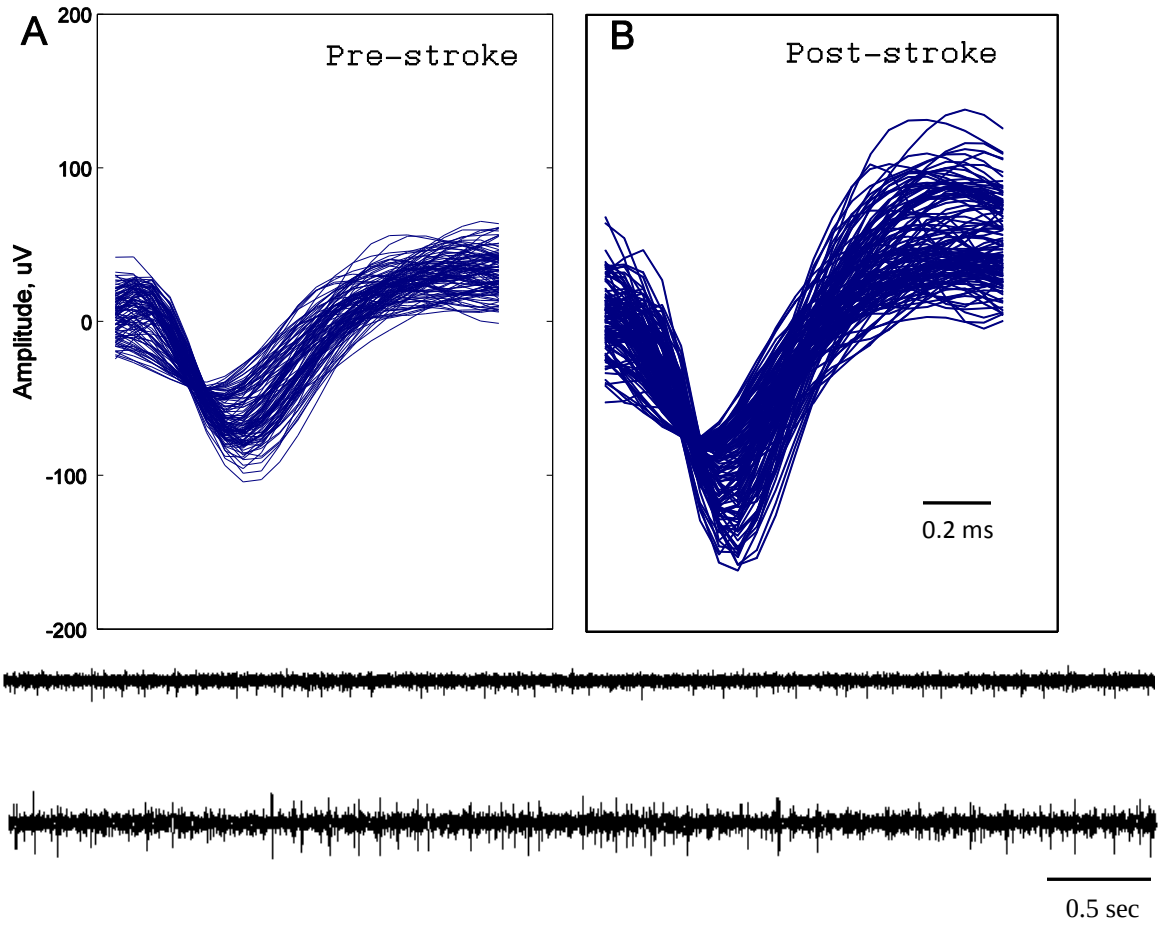

Figure 7: Raw data of Electrode V, showing differences between pre-and post-stroke subpopulation excitability. *A*: Pre-stroke sample of action potentials; *B*: Post-stroke sample of action potentials; *C, D*: Pre- and post-stroke raw data samples, respectively. Increased, persistent neuronal excitability was found in all subpopulations as a result of stroke induction. The greatest excitability increase is presented here from Electrode V.

Post-stroke subpopulation neural behavior during task

While the small focal stroke did not significantly affect the daily life activities of the animal, visible difficulty was observed during the initial grasp of the robot handle. As shown in Figure 8, the change in subpopulation neural activity as a result of stroke induction differed for each electrode placement. The subpopulation observed from Electrode V maintained the same velocity path and averaged IFR, while the subpopulation-averaged IFR increased from pre-stroke to post-stroke in subpopulations of Electrodes IV and VI in differing degrees. The subpopulation averaged IFR of Electrode I placement shows an initial position-dependent increase in averaged IFR as a result of the stroke, but decreases to less than pre-stroke IFR with trial progression. This comparative IFR decrease is

suggested to be due to the ischemic penumbral region (Wester *et al.* 1995) extending to the area of Electrode I. Although the subpopulation of neurons from Electrode V did not exhibit a considerable change in averaged IFR as a result of cortical infarction, as shown in Figure 7, the subpopulation of neurons exhibited the greatest increase in neuronal excitability. In a study using photothrombosis to induce cortical infarction, Schiene *et al.* (1996) reported a similar increased neuronal excitability following stroke induction.

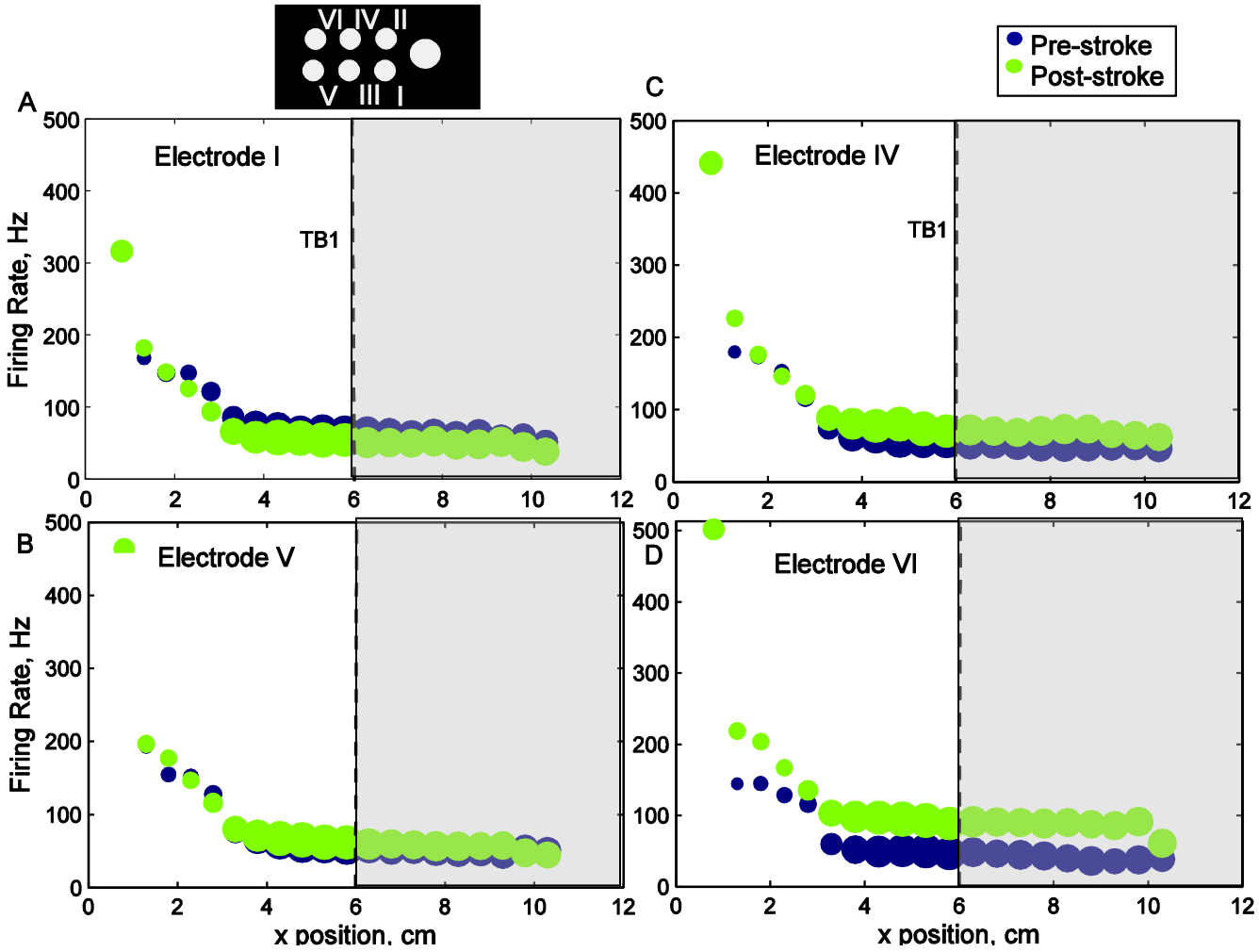

Figure 8: Averaged differences pre-to post-stroke for 4 electrodes of a single rat. Pre-and post-stroke average IFR per 5 mm from Rat I. Size of bubbles are directly proportional to velocity, which was not considerably affected by stroke. *A-D* show electrodes I, IV, V, VI, respectively (refer to locations in above electrode placement schematic). (D) Electrode VI placement. Blue indicates pre-stroke IFR. Green indicates post-stroke IFR. Post-stroke IFR suggests a relationship with the distance of the electrode from the focal infarct area as can be seen from the schematic drawing of electrode positions.

DISCUSSION

Haptic systems as animal behavioral tasks

The current system was designed and developed to explore the possibilities and benefits of using a haptic interface as the foundation for animal behavioral tasks. The system described in this study is a one-dimensional haptic behavioral task, with a high kinematic sampling rate, that incorporated dynamic constraints as a method of reducing path variability and increasing movement repeatability. As illustrated in Figure 4B, the task was repeatable from day-to-day. The high kinematic sampling rate allowed synchronization of the kinematic and neuro-electrophysiological data to provide precise information on the relationship between neural behavior and movement parameters. Since the system uses a haptic interface and programming language, the behavioral task can be easily altered to target specific rate-influencing parameters or adapt to changing post-injury rehabilitation needs.

Rats were used in this preliminary study. However, since haptic systems are commonly used in human motor rehabilitation, spatial and dynamic ranges are easily adaptable to the requirements of monkeys. The neural recording system used in this study has servers that allow client programs, such as programming languages, to access system hardware and previously recorded neural data, affording ease in coupling of the neural recording system with the haptic interface.

Although neural activity was recorded during the initial reach and grasp of the robot handle, movement information was only available once the robot handle became non-stationary. Analyzing the initial reach (pre-handle movement onset) was difficult and therefore was excluded from this study due to the focus having been on establishing movement repeatability of a simplified haptic behavioral task. However, it is supposed that incorporating electromyography (EMG) to obtain detailed targeted muscle force production characteristics or motion tracking for joint angle reconstruction (Donoghue *et al.* 1992; McKiernan *et al.* 1998; Vargas-Irwin *et al.* 2010) on a larger animal such as a monkey would provide another dimension of information in movement, in addition to providing information on the spatiotemporal relationship between movement and neural behavior during the initial reach.

Subpopulation neural behavioral response to learned behavior

As previously stated, the animals used in the current preliminary study were overtrained in the behavioral task for ten to eleven months before electrode implantation. On a subpopulation level, neural activity in relationship to the task was stable throughout the day-to-day study. Additionally, subpopulation neural activity was observed as unresponsive to a progressively increasing opposing force and subsequent change in velocity output during trial progression. This is suggested to be the result of the non-complex behavioral task evolving into a learned behavior. However, since subpopulation level activity was observed in this study, it is also possible that activity from a single neuron was affected by change in force or velocity but was not detected on a larger scale. However, the results presented in this thesis are preliminary and further study and more complex tasks are required to better understand the relationship between neural activity in an animal completing an overtrained task.

Effects of cortical infarction on subpopulation neural behavior

The stroke induced in this study was not severe enough to inhibit daily activities of the animal. It is probable that the small infarct area is a contributing factor to the pre-stroke subpopulation firing tendency, in relation to the behavioral task, to return to pre-movement baseline being maintained post-stroke. The reason for increased neuronal excitability of Electrode V, coupled with a small increase, relative to Electrodes IV and VI, in change in subpopulation neural firing in relation to the task is unknown. However, it may be due to the electrode being located outside of the forelimb representation area. Further study is needed to gain more insight into the results of stroke induction on the neural behavior of M1 neurons in an animal completing an overtrained behavioral task, but the results provided in this thesis offer insight into the effects of focal M1 infarction on peri-infarct subpopulation neural behavior, where post-stroke IFR reduces activity near to the lesion (Figure 8A), and then increases for distant electrodes (Figure 8C and D). Such a relation is consistent with the idea of an irreparably damaged area surrounded by an adjacent penumbral region that recovers and even has

heightened activity post ischemia (Wester *et al*. 1995). While the data presented here is quite sparse, this sheds light on the possibility of studying these regions in the future with this type of preparation.

Future implications

The system presented in this study was able to achieve movement repeatability of an animal performing a behavioral task by incorporating haptics and utilizing dynamic constraints, in addition to providing higher spatiotemporal resolution via high sampling rates. Expanding the haptic system to include multi-dimensional behavioral tasks while maintaining movement repeatability would require inclusion of more dynamic constraints and creation of a task-specific haptic environment. However, modifications to the virtual haptic environment and dynamics only necessitate changes in programming code; thereby affording ease-of-use and adaptability to independent changes in targeted kinematic or dynamic parameters or change in user needs as a result of motor cortical injury.

Overtrained, non-sequential behavioral tasks can develop into learned behaviors, which results in an increased threshold for neural activity baseline deviation in response to change in neural behavioral-influencing parameters. On the subpopulation level, with respect to handle position and time, a persistent firing trend was observed from each electrode in each animal. Observing activity of single neurons and their correlation with surrounding units may provide more detailed information about the relationship between neural activity and its response to learned behaviors. Additionally, the effects of a small focal cortical infarction on an overtrained animal revealed changes in comparative pre-stroke subpopulation activity while maintaining the firing trend present before the infarction. This needs to be further studied, as results could offer information about the neural-behavioral relationship that leads to more defined and individualized motor retraining methods.

In summary, a brain-machine interface as a motor rehabilitation system, with the capabilities to provide high spatiotemporal resolution and independent modification of spatial, kinematic, and dynamic parameters has been introduced in this study. Additionally, preliminary findings on the

subpopulation neural behavioral response to a learned behavior showed that M1 activity might become desensitized to incrementing changes in neural behavioral-influencing parameters as a result of overtraining. Finally, the effects of focal M1 infarction on subpopulation activity, which illustrated distance-dependent changes in neuronal excitability of an overtrained animal completing a behavioral task, showed visible relationships with pre-infarct activity. These effects could provide a foundation of knowledge that is used to design motor rehabilitation treatments incorporating post-stroke cortical stimulation that leads to targeted stimulation of peri-infarct areas and, in combination with behavioral rehabilitation, improvements in motor function recovery.

BIBLIOGRAPHY

Ashe, J. (1997). Force and the motor cortex. *Behavioural Brain Research , 86* (1), 1-15.

Ashe, J., & Georgopoulos, A. (1994). Movement Parameters and Neural Activity in Motor Cortex and Area 5. *Cereb Cortex , 4*, 590-600.

Ballermann, M., Tompkins, G., & Whishaw, I. Q. (2000). Skilled forelimb reaching for pasta guided by tactile input in the rat as measured by accuracy, spatial adjustments, and force. *Behav Brain Res , 109* (1), 49-57.

Chapin, J. K., Moxon, K. A., Markowitz, R. S., & Nicolelis, M. A. (1999). Real-time control of a robot arm using simultaneously recorded neurons in the motor cortex. *Nat Neurosci , 2*, 664–670.

Chiganos, T. C., Jensen, W., & Rousche, P. J. (2006). Electrophysiological response dynamics during focal cortical infarction. *J. Neural Eng. , 3*, L15–L22.

Ding, C., & He, X. (2004). K-means Clustering via Principal Component Analysis. *Proceedings of the 21st International Conference on Machine Learning* (pp. 225–232). New York: ACM Press.

Donoghue, J. P., Leibovic, S., & Sanes, J. N. (1992). Organization of the forelimb area in squirrel monkey motor cortex: representation of digit, wrist, and elbow muscles. *Exp Brain Res. , 89* (1), 1-19.

Evarts, E. V. (1966). Pyramidal tract activity associated with a conditioned hand movement in the monkey. *J. Neurophysiol , 29* (6), 1011-1027.

Georgopoulos, A. P., Ashe, J., Smyrnis, N., & Taira, M. (1992). The motor cortex and the coding of force. *Science , 256*, 1692-1695.

Georgopoulos, A. P., Kalaska, J. F., & Massey, J. (1981). Spatial trajectories and reaction times of aimed movements: Effects of practice, uncertainty and change in target location. *J. Neurophysiol , 46* (4), 725–743.

Georgopoulos, A. P., Kalaska, J. F., Caminiti, R., & Massey, J. T. (1982). On the relations between the direction of two-dimensional arm movements and cell discharge in primate motor cortex. *J. Neurosci , 2* (11), 1527-1537.

Holden, M. (2005). Virtual Environments for Motor Rehabilitation: Review. *CyberPsychology & Behavior , 8* (3).

Jensen, W., & Rousche, P. J. (2006). On variability and use of rat primary motor cortex responses in behavioral task discrimination. *J. Neural Eng. , 3*, L7–L13.

Kargo, W. J., & Nitz, D. A. (2004). Improvements in the Signal-to-Noise Ratio of Motor Cortex Cells Distinguish Early versus Late Phases of Motor Skill Learning. *J. Neurosci. , 24* (24), 5560-5569.

Karni, A., Meyer, G., Rey-Hipolito, C., Jezzard, P., Adams, M. M., Turner, R., et al. (1998). The acquisition of skilled motor performance: Fast and slow experience-driven changes in primary motor cortex. *Proc Natl Acad Sci USA , 95* (3), 861–868.

Kleim, J. A., Barbay, S., & Nudo, R. J. (1998). Functional Reorganization of the Rat Motor Cortex Following Motor Skill Learning. *J Neurophysiol , 80* (6), 3321-3325.

Laubach, M., Wessberg, J., & Nicolelis, M. A. (1998). Cortical ensemble activity increasingly predicts behaviour outcomes during learning of a motor task. *Nature , 405*, 567-571.

Lewicki, M. S. (1998). A review of methods for spike sorting: the detection and classification of neural action potentials. *Comput. Neural Syst. , 9*, R53–R78.

Lewicki, M. S. (1998). A review of methods for spike sorting: the detection and classification of neural action potentials. *Comput. Neural Syst. , 9*, R53–R78.

Lu, X., & Ashe, J. (2005). Anticipatory Activity in Primary Motor Cortex Codes Memorized Movement Sequences. *Neuron, , 45*, 967–973.

Matsuzaka, Y., Picard, N., & Strick, P. L. (2007). Skill Representation in the Primary Motor Cortex After Long-Term Practice. *J Neurophysiol , 97*, 1819–1832.

McKeirnan, B. J., Marcario, J. K., Karrer, J. H., & Cheney, P. D. (1998). Corticomotoneuronal postspike effects in shoulder, elbow, wrist, digit, and intrinsic hand muscles during a reach and prehension task. *J. Neurophysiol. , 80*, 1961–1980.

Metz, G. A., & Whishaw, I. Q. (2000). Skilled reaching an action pattern: stability in rat (Rattus norvegicus) grasping movements as a function of changing food pellet size. *Behav Brain Res , 116* (2), 111-122.

Moran, D., & Schwartz, A. (1999a). Motor Cortical Representation of Speed and Direction During Reaching. *J. Neurophysiol , 82*, 2676-2692.

Neafsey, E. J. (1990). The complete ratunculus: output organization of layer V of the cerebral cortex. In B. Kolb, & R. C. Tees (Eds.), *The Cerebral Cortex of the Rat* (pp. 197–212). Cambridge, MA: MIT Press.

Nudo, R. J., Milliken, G. W., Jenkins, W. M., & Merzenich, M. M. (1996). Use-dependent alterations of movement representations in primary motor cortex of adult squirrel monkeys. *J. Neurosci. , 16*, 785–807.

Nudo, R. J., Plautz, E. J., & Frost, S. B. (2001). Role of adaptive plasticity in recovery of function after damage to motor cortex. *Muscle Nerve , 24*, 1000–1019.

Paninski, L., Fellows, M. R., Hatsopoulos, N. G., & Donoghue, J. P. (2004). Spatiotemporal Tuning of Motor Cortical Neurons for Hand Position and Velocity. *J Neurophysiol , 91*, 515–532.

Plautz, E. J., Milliken, G. J., & Nudo, R. J. (2000). Effects of Repetitive Motor Training on Movement Representations in Adult Squirrel Monkeys: Role of Use versus Learning. *Neurobiol Learn Mem , 74* (1), 27-55.

Sanes, J. N., & Donoghue, J. P. (2000). Plasticity and Primary Motor Cortex. *Annu Rev Neurosci , 23*, 393-415.

Schiene, K., Bruehl, C., Zilles, K., Qu, M., Hagemann, G., Kraemer, M., et al. (1996). Neuronal Hyperexcitability and Reduction of GABAA-Receptor Expression in the Surround of Cerebral Photothrombosis. *J Cerebr Blood Flow Metab , 16*, 906–914.

Sergio, L. E., Hamel-Paquet, C., & Kalaska, J. F. (2005). Motor Cortex Neural Correlates of Output Kinematics and Kinetics During Isometric-Force and Arm-Reaching Tasks. *J Neurophysiol , 94* (4), 2353-2378.

Vargas-Irwin, C. E., Shakhnarovich, G., Yadollahpour, P., Mislow, J. M., Black, M. J., & Donoghue, J. P. (2010). Decoding Complete Reach and Grasp Actions from Local Primary Motor Cortex Populations. *J. Neurosci. , 30* (29), 9659–9669.

Wang, W., Chan, S. S., Heldman, D. A., & Moran, D. W. (2010). Motor Cortical Representation of Hand Translation and Rotation during Reaching. *J. Neurosci. , 30* (3), 958 –962.

Wester, P., Watson, B. D., Prado, R., & Dietrich, W. D. (1995). A Photothrombotic `Ring' Model of Rat Stroke-in-Evolution Displaying Putative Penumbral Inversion. *Stroke , 26*, 444-450.

Whishaw, I. Q., & Pellis, S. M. (1990). The structure of skilled forelimb reaching in the rat: A proximally driven movement with a single distal rotatory component. *Behav Brain Res , 41* (1), 49-59.

Williams, J. C., Rennaker, R. L., & Kipke, D. R. (1999). Long-term neural recording characteristics of wire microelectrode arrays implanted in cerebral cortex. *Brain Res. Protocols , 4*, 303-313.

Wood, F., Black, M. J., Vargas-Irwin, C., Fellows, M., & Donoghue, J. P. (2004). On the Variability of Manual Spike Sorting. *IEEE Trans Biomed Eng , 51* (6), 912-918.

VITA

NAME: Ashley Victoria Greene

EDUCATION: B.S.E., Bioengineering, Arizona State University, Tempe, Arizona, 2007

M.S., Neural Engineering, University of Illinois at Chicago, Chicago, Illinois, 2011

PROFESSIONAL MEMBERSHIP: Biomedical Engineering Society

ABSTRACTS: Ashley V. Greene, Patrick J. Rousche, Milan Ramaiya and James Patton.: Neural feedback from the motor cortex and spatial forelimb information during robot rehabilitation using a rat. Abstr. Annu. Meet. Biomed. Eng. Soc. 2009.

Ashley V. Greene, Patrick J. Rousche, Milan Ramaiya and James Patton.: A system for simultaneous neural recording and spatial forelimb tracking during robot rehabilitation. Abstr. Annu. Meet. Soc. for Neurosci. 2009.